Quantum reflection of He* on silicon

Hilmar Oberst,[1] Yoshihisa Tashiro,[1] Kazuko Shimizu,[1,2] and Fujio Shimizu[1,3]

[1]*Institute for Laser Science, University of Electro-Communications, Chofu-shi, Tokyo 182-8585, Japan*
[2]*Department of Applied Physics and Chemistry, University of Electro-Communications, Chofu-shi, Tokyo 182-8585, Japan*
[3]*NTT Basic Research Laboratories, NTT Corporation, and CREST, Morinoshita-Wakamiya, Atsugi 243-0198, Japan*

A cold beam of He* ($2\,^3S_1$) atoms is used at grazing incidence to study the quantum reflection on a flat polished silicon surface. We measure the reflectivity as a function of the normal incident velocity component between 3 and 30 cm/s. Our result is in reasonable agreement with a calculation of the attractive van der Waals surface potential using the dielectric function of Si and the dipole polarizability of He*. We discuss the influence of the conductivity and of a thin oxide layer on the potential. By comparing our data to those previously measured with Ne* atoms, we are also able to confirm the scaling of the reflectivity with atomic mass.

I. INTRODUCTION

Optics has been a main source of inspiration for many experiments with atomic waves. The analogy of phenomena observed with photons and atoms is of course largely based on the fact that equivalent equations govern their propagation. One of the consequences of this wave equation is the reflection at an abrupt change in the (generally complex) index of refraction, or correspondingly of the interaction potential, regardless of the sign of change. In the case of atoms, such reflections have been called "quantum reflection" and predicted to occur when slow atoms approach the steep slope of the van der Waals attraction near liquid and solid surfaces. It has been experimentally observed with slow atoms reflected on liquid helium surfaces [1–6] and more recently also on solid surfaces [7–10]. The study of atom reflections at attractive potentials, in particular at solid surfaces, has seen a considerable increase in interest recently, both as a means to study the atom-surface potentials and in view of possible applications in atom optics [11–15]. Atom reflectors based on solid surfaces are inherently stable, accurate, and nearly dispersionless and they can be made very large. The reflection is coherent as long as the wavelength of the incident wave is large compared to the surface roughness. This condition is easily realized with polished surfaces and laser-cooled atoms or at grazing incidence. The main disadvantage of solid surface atom mirrors is their low reflectivity which still strongly limits their applicability; however, some progress has been made in this respect by preparing atoms in a Bose-Einstein condensate with extremely low incident velocities [10], or by using microfabricated surface structures [16,17].

We report here on the experimental observation of quantum reflection of laser-cooled metastable helium atoms on a silicon surface at grazing incidence. This is a continuation of our work with metastable neon atoms [8] and we are able to directly confirm the scaling of the reflectivity with atomic mass. The helium-silicon system offers the advantage that all the material properties are very well known. However, a peculiarity arises due to the fact that silicon is an intermediate case between a perfect conductor and a pure dielectric, which

requires an additional analysis when calculating the interaction potential. We present here a detailed analysis of the van der Waals potential in the case of a poor conductor. The interaction potential between a metastable helium atom and a doped silicon surface is calculated. In addition, we discuss the influence of an oxide surface layer on the potential shape.

II. INTERACTION POTENTIAL

At a distance large compared to the size of the atom, the interaction potential between an atom and the solid is the dipole attraction, $U(r) = -C_3/r^3$, where r is the distance from the surface [18,19]. At a distance larger than the wavelengths of atomic transitions, however, retardation effects become important and the potential changes to $U(r) = -C_4/r^4$ [20,21]. Several authors have derived general expressions for the interaction potential between an atom and a solid [22–24]. We use in the following the formula given in Refs. [24,25] (SI units are used throughout):

$$U(r) = -\frac{\hbar}{8\pi^2\epsilon_0 c^3} \int_0^\infty d\xi \, \alpha(i\xi) \times \int_1^\infty dp \, \xi^3 e^{-2\xi rp/c} H(p, \epsilon(i\xi)),$$

(1)

where the path of integration over the frequency ξ has been shifted to the complex plane, and

$$H(p, \epsilon) = \frac{s-p}{s+p} + (1 - 2p^2)\frac{s - \epsilon p}{s + \epsilon p},$$

(2)

$$s = \sqrt{\epsilon - 1 + p^2}.$$

(3)

Here, ϵ and α are the frequency-dependent and general complex dielectric constant of the solid and the dipole polarizability of the atom, respectively.

Note that due to the exponential factor in Eq. (1) and since $p \geqslant 1$, the main contribution to the integral is limited to a frequency region where

$$\xi < \omega_r \equiv \frac{c}{r}.$$

(4)

Without knowledge of both $\alpha(i\omega)$ and $\epsilon(i\omega)$, the potential cannot be further calculated. However, it is possible to derive expressions for the potential in the limiting cases of very small and very large r, which are usually given in the literature. We briefly repeat them below.

(i) For $r \to 0$, the integral over p in Eq. (1) has a simple asympotic form,

$$\int_1^\infty dp\ \xi^3 \exp(-2\xi rp/c) H(p, \epsilon(i\xi)) \to \frac{c^3}{2r^3} \frac{\epsilon(i\xi)-1}{\epsilon(i\xi)+1} \quad (5)$$

and we can write $U(r) = -C_3/r^3$ with

$$C_3 = \frac{\hbar}{16\pi^2\epsilon_0} \int_0^\infty d\xi \alpha(i\xi) \frac{\epsilon(i\xi)-1}{\epsilon(1\xi)+1}. \quad (6)$$

(ii) For $r \to \infty$, only very low frequencies contribute to the integral. In practice, it is sufficient to go to a distance l so that c/l is lower than the smallest significant frequency in the absorption spectrum of the atom, and replace $\alpha(i\xi)$ by the static dipole polarizability $\alpha(0)$. For a perfect conductor $\epsilon(i\omega) \to \infty$ and Eq. (2) simplifies to $H(p,\epsilon) \to 2p^2$. The double integral in Eq. (1) is then readily evaluated to be $3c^4\alpha(0)/(4r^4)$ and we obtain

$$U(r) = -\frac{C_4}{r^4} \quad \text{with} \quad C_4 = \frac{3\hbar c\alpha(0)}{32\pi^2\epsilon_0}. \quad (7)$$

For a dielectric with frequency-independent dielectric constant ϵ, a similar derivation leads to the result [25,26]

$$U(r) = -\frac{C_4}{r^4} \frac{\epsilon-1}{\epsilon+1} \phi(\epsilon). \quad (8)$$

An analytical expression for the function $\phi(\epsilon)$ is given in Ref. [25], Eq. (21).

When both C_3 and C_4 are known, the potential is in practice often approximated by the analytical form

$$U(r) = -\frac{C_3}{r^3} \beta(r/l) \quad \beta(x) = \frac{1}{1+x}, \quad (9)$$

where $l = C_4/C_3$.

III. QUANTUM REFLECTION OF ATOMS AT THE van der WAALS POTENTIAL

A matter wave is reflected when the potential changes sufficiently abruptly within one de Broglie wavelength. This condition of impedance mismatch can be expressed as

$$\frac{1}{k^2} \left| \frac{dk}{dr} \right| > 1, \quad \text{where} \quad k(r) = \sqrt{k_0^2 - 2MU(r)/\hbar^2} \quad (10)$$

is the local wave vector, with k_0 the wave vector of the incident atom with mass M. The condition can be formulated more rigorously by introducing a so-called "Badlands" function $B(r)$ [13]: If $B(r) \ll 1$, the motion of the particle is well described using the notion of a trajectory in the WKB approximation. For $B(r) \gtrsim 1$, this approximation breaks down and quantum reflection is expected to occur. For a potential

$U(r) = -C_n/r^n$, $n > 2$, the function $B(r)$ has a maximum near the distance r_0 where the absolute value of the potential equals the incident energy of the atom, i.e., $|U(r_0)| = \hbar^2 k_0^2 / 2M$. The reflection occurs mainly at this point [3].

In our experiment, we used metastable helium atoms incident on a silicon surface with a normal incident velocity component between about 3 and 30 cm/s. The corresponding de Broglie wavelengths range from 0.3 to 2 μm, and the atoms are reflected at a distance from the surface varying between 150 and 300 nm. The reflectivity of the atoms will therefore be predominantly determined by the strength of the potential in this region.

The Schrödinger equation with the potential $U(r) = -C_n/r^n$ can be written in dimensionless form by scaling r with $r_s = (MC_n/\hbar^2)^{1/(n-2)}$, and the incident kinetic energy with $E_s = \hbar^2/(Mr_s^2) =: Mv_s^2$. We can therefore define the scale of the incident velocity as

$$v_s = \frac{\hbar}{M} \left(\frac{\hbar^2}{MC_n} \right)^{1/(n-2)}. \quad (11)$$

The reflectivity of atoms on a solid surface $R = R(v_0/v_s)$ approaches 1 when the incident velocity $v_0 \to 0$ but decreases rapidly with increasing incident velocity. With the exception of helium, the reflectivity is typically below 1% for velocities above a few cm/s. Because v_s scales with M^{-2} for $n = 3$, and with $M^{-3/2}$ for $n = 4$, lighter atoms are reflected more efficiently. Similarly, a smaller potential constant C_n should lead to a higher reflectivity. Since C_n is roughly proportional to the density, a material with lower density will be a better reflector.

The scaling law might lead to the paradoxical conclusion that the reflectivity will approach unity as C_n approaches zero. This property of the scaling law is of course a mathematical consequence of the divergence of the potential at $r \to 0$. In reality, the potential will change its shape, typically to some short-range repulsive potential well, as the atom approaches the surface. It can, however, be argued more generally that, if the long-range van der Waals interaction is reduced, any short-range surface potential will look like a potential step to a sufficiently slow incident atom, which will therefore be reflected coherently.

IV. THE van der WAALS POTENTIAL FOR POOR CONDUCTORS

The electrical conductivity is one of the most strongly varying properties of solids. Whereas for metals the static conductivity σ_0 is as high as 6.2×10^5 $(\Omega\,\text{cm})^{-1}$ for silver, it is less than $\sigma = 10^{-14}$ $(\Omega\,\text{cm})^{-1}$ for an electrical insulator. Semiconductors have conductivities that typically range from 10^{-9} to 10^2 $(\Omega\,\text{cm})^{-1}$ and depend strongly on temperature and impurities. In the derivation of the interaction potential between an atom and a solid, we have used the notions of a perfect conductor ($\epsilon = \infty$) and of a dielectric. However, in the case of a semiconductor, the question arises whether and in which range of electrical conductivities the models of a perfect conductor and of a dielectric are still applicable, and how the potential changes in the intermediate

region. To our knowledge, this question has never been discussed in the literature.

Schwinger *et al.* [27] and Hargreaves [28] briefly considered the case of an imperfect metal by using the expression $\epsilon(\omega) = 1 - \omega_p^2/\omega^2$, where $\omega_p^2 = ne^2/(m^*\epsilon_0)$ is the plasma frequency squared. The conductor is imperfect in the sense that at high frequencies (typically in the infrared or higher spectral region), the dielectric function will eventually drop to 1. The resulting first-order deviation of the van der Waals potential from the infinite dielectric constant result was calculated. Recently, the effect of a finite conductivity of the metal surface on the Casimir-Polder interaction has been discussed in more details by Babb *et al.* [29], who also calculate the potential between a gold wall and He*, Na, and Cs atoms taking into account the finite conductivity of the metal, the dynamic polarizability of the atom, and nonzero temperature. For metals, the finite conductivity usually leads to a small correction that is, however, not negligible in precision experiments.

In the following, we will discuss the case when the conductivity is not only finite but small, i.e., the transition from a metal to a dielectric. A conducting material is characterized by a resonance of the dielectric function at $\omega = 0$. If we separate the part of the dielectric function that is due to the presence of "free" charges, we can generally write [30]

$$\epsilon(\omega) = \epsilon_b + i\frac{\sigma(\omega)}{\epsilon_0\omega}. \tag{12}$$

Here, ϵ_b denotes the background dielectric function, which is usually nearly constant at low frequencies, and the conductivity σ can be expressed as

$$\sigma(\omega) = \frac{ne^2}{m^*(\gamma_0 - i\omega)} = \frac{\sigma_0}{1 - i\omega/\gamma_0}, \tag{13}$$

where n is the number of free charges per unit volume, m^* the effective mass of the charged particle, γ_0 is a damping rate, and $\sigma_0 = ne^2/(m^*\gamma_0)$ the static conductivity. We therefore write the imaginary-frequency dielectric function as

$$\epsilon(i\omega) = \epsilon_b + \frac{1}{\omega/\omega_\sigma + \omega^2/\omega_p^2}, \tag{14}$$

where we have introduced the frequency $\omega_\sigma = \sigma_0/\epsilon_0$, and $\omega_p^2 = \omega_\sigma\gamma_0 = ne^2/(m^*\epsilon_0)$ is again the plasma frequency squared mentioned above. We conclude that the solid behaves like a conductor for frequencies below both ω_σ and ω_p, whereas it behaves like a dielectric for frequencies above either ω_σ or ω_p.

We have seen above [Eq. (1)] that, in the calculation of the van der Waals potential, the main contribution comes from the frequency region $\omega < \omega_r = c/r$, where r is the distance from the surface. We have also said in the previous section that slow atoms are reflected at distances in the order of a few hundred nanometers. The corresponding frequency region that we have to consider in the evaluation of the potential therefore extends from zero up to the optical region: $\omega_r \approx 10^{15}$ s^{-1}. If ω_σ or ω_p are equal to or higher than ω_r, then ϵ will be large over the relevant frequency region, and the potential will be that of a perfect conductor. If, on the con-

trary, ω_σ, $\omega_p \ll \omega_r$, then $\epsilon(i\omega) \approx \epsilon_b$ and the potential will be that of a dielectric.

For a typical metal, ω_s and ω_p are very large compared to $\omega_r = c/r$ and the solid behaves like an almost perfect conductor for an atom reflected by the van der Waals potential. The finite conductivity leads only to a small correction at very small distances from the surface.

If the density of charges is reduced, the dielectric function will eventually approach that of an insulator. We can estimate the order of magnitude of the number of charges per volume n at which this transition occurs, by setting $\omega_r = c/r \approx \omega_p = ne^2/(m_e\epsilon_0)$, where m_e is the mass of the electron. For $r = 0.5$ μm, we obtain $n \approx 10^{19}$ cm^{-3}. Assuming that the damping rate $\gamma_0 = 10^{13}$ s^{-1}, which is a typical value for metals and many semiconductors at room temperature, the corresponding static conductivity $\sigma_0 \approx 10^3$ (Ω cm)$^{-1}$.

The conductivities of pure silicon and germanium at room temperature are 3.8×10^{-6} (Ω cm)$^{-1}$ and 2.3×10^{-2} (Ω cm)$^{-1}$, respectively. At a distance from the surface in the order of 0.5 μm, the van der Waals potential of both materials will be that of a dielectric, in spite of the presence of free charges. By doping the material, the conductivity can be increased by several orders of magnitude. Highly doped silicon can reach conductivities of 10^2 (Ω cm)$^{-1}$ or higher, and small deviations from the pure-dielectric potential are expected.

In conclusion, we have analyzed the influence of the electrical conductivity on the van der Waals interaction potential between a solid surface and an atom. For metals, the approximation of a perfect conductor is very good in most cases, and the finite conductivity causes small deviations only at short distances from the surface. On the other hand, the conductivities of semiconductors are generally so low— even at high doping concentrations—that the interaction potential is mainly determined by the dielectric properties of the semiconductor, and the presence of free charges leads only to small corrections at larger distances.

V. THE CASE OF He* AND SILICON

We have concluded in the previous section that for silicon, the dielectric properties will dominate over the effect of free charges. That means that we will have to consider the dielectric function of silicon in the calculation of the van der Waals potential. The interaction potential between the helium atom and the solid is the same for all metals but not for dielectrics. We will calculate the potential for both cases and compare them later to our experimental results.

The imaginary-frequency dipole polarizabilities of the metastable states of He have been calculated by several authors, the precision increasing over time [26,31,32]. For the $2\,^3S_1$ state, the function can be quite well approximated by a simple one-oscillator model for the atom

$$\alpha(i\omega) \approx \frac{\alpha(0)}{1 + (\omega/\omega_a)^2}, \tag{15}$$

with $\alpha(0) = 5.204 \times 10^{-39}$ F m^2 (315.631 atomic units) and $\omega_a = 1.793 \times 10^{15}$ s^{-1} [33].

For a perfectly conducting surface, we assume $\epsilon = \infty$ and calculate the potential by integrating Eq. (6). Using the one-oscillator model for $\alpha(i\omega)$ [Eq. (15)], we obtain

$$C_3^\infty \approx \frac{\hbar\alpha(0)\omega_a}{32\pi\epsilon_0} = 1.1 \times 10^{-48} \text{ J m}^3, \qquad (16)$$

which is about 10% below the exact value given in Ref. [26],

$$C_3^\infty = 1.2281 \times 10^{-48} \text{ J m}^3 \ (1.900\,92 \text{ atomic units}). \qquad (17)$$

This value is reproduced within a relative error below 1% by integrating Eq. (6) using the exact values for $\alpha(i\omega)$ given in Refs. [31,32]. Similarly, we obtain for the coefficient of the retarded potential using Eq. (7)

$$C_4^\infty = 1.765 \times 10^{-55} \text{ J m}^4 \ (5163 \text{ atomic units}). \qquad (18)$$

In order to calculate the potential for the silicon surface, we have to include the dielectric properties of the semiconductor. Fortunately, the dielectric function of silicon is known over nearly the entire spectral range [34]. If we neglect details, an oscillator model is appropriate to describe its main characteristics. Vidali and Cole [33] pointed out that the imaginary-frequency dielectric constant of many solids can be approximated by the expression

$$\frac{\epsilon(i\omega) - 1}{\epsilon(i\omega) + 1} \approx \frac{\epsilon(0) - 1}{\epsilon(0) + 1}\frac{1}{1 + (\omega/\omega_s)^2}. \qquad (19)$$

For silicon, they give $\epsilon(0) = 11.7$ and $\omega_s = 1.78 \times 10^{16} \text{ s}^{-1}$, in agreement with the values of Ref. [34].

Since ω_s is about one order of magnitude larger than ω_a, the dielectric function of silicon is nearly constant over the entire range where $\alpha(i\omega)$ is considerably larger than zero [see Fig. 1(a)]. We can therefore expect that using Eq. (6) with $\epsilon(i\omega) = \epsilon(0)$ is a good approximation, i.e.,

$$C_3^{\text{Si}} \approx \frac{\epsilon(0) - 1}{\epsilon(0) + 1}C_3^\infty = 1.03 \times 10^{-48} \text{ J m}^3. \qquad (20)$$

Integration of Eq. (6) using the frequency-dependent dielectric function from Eq. (19) and the dynamic dipole polarizability of He* from Refs. [31,32] leads to an additional correction of about 15%,

$$C_3^{\text{Si}} = 0.85\frac{\epsilon(0) - 1}{\epsilon(0) + 1}C_3^\infty = 8.8 \times 10^{-49} \text{ J m}^3. \qquad (21)$$

Similarly, we obtain for the C_4 coefficient between the He* atom and the silicon surface

$$C_4^{\text{Si}} = C_4^\infty\frac{\epsilon(0) - 1}{\epsilon(0) + 1}\phi(\epsilon(0))$$

$$= C_4^\infty \times 0.843 \times 0.808 = 1.202 \times 10^{-55} \text{ J m}^4. \qquad (22)$$

The transition from the unretarded to the retarded regime takes place at the distance $l = C_4^{\text{Si}}/C_3^{\text{Si}} = 137$ nm.

A word of caution is required at this point: we have introduced the constant C_4 in the limit $r \to \infty$, with the consequence that only the static dielectric function contributes to the interaction potential. Since the presence of free charges
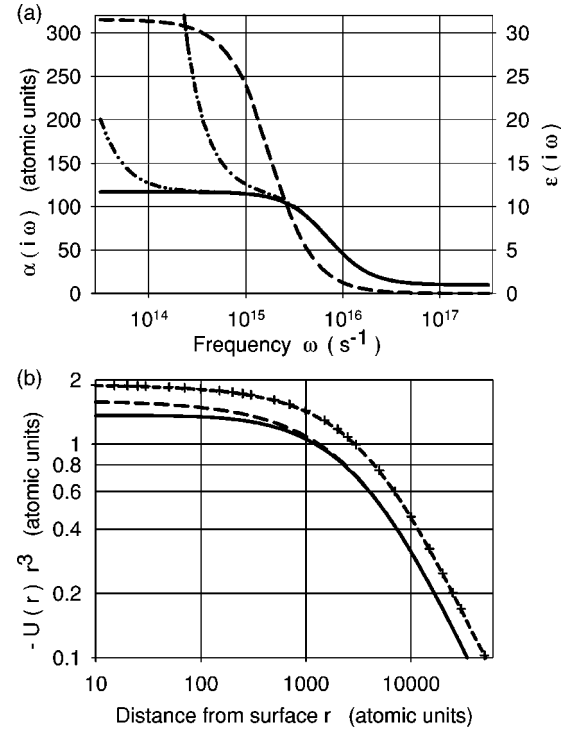

FIG. 1. (a) The imaginary-frequency dipole polarizability $\alpha(i\omega)$ of He* $(2\,^3S_1)$ taken from Refs. [31,32] (dashed line) and the dielectric function $\epsilon(i\omega)$ of silicon (solid line) calculated using Eq. (19) and the values from Ref. [33]. We also show the dielectric function of doped silicon with a plasma frequency $\omega_p = 10^{14} \text{ s}^{-1}$ (dash-dot-dot) and $\omega_p = 10^{15} \text{ s}^{-1}$ (dash-dot). The presence of free charges leads to a resonance at zero frequency. (b) The van der Waals potential between a He* atom and a silicon surface. The short-dashed line shows the potential in the case of a perfectly conducting surface. It has been calculated using Eq. (1) and the He* dipole polarizability plotted in (a). This calculation reproduces the values given by Yan and Babb [26] (crosses) with a relative error below 1%. The dashed line is the potential calculated for a dielectric with the frequency-independent dielectric function $\epsilon = 11.7$ and the solid line is the potential calculated using the frequency-dependent dielectric function of undoped silicon. The latter differ only at very short distances from the surface, where the high-frequency behavior of $\epsilon(i\omega)$ must be considered.

leads to a resonance of the dielectric function at $\omega = 0$, C_4 will then always assume the value of a perfect conductor. However, for a poor conductor, the distance r where this limit is valid might be impractically large. The expression for C_4^{Si} given above is valid in the region $c/\omega_a < r < c/\omega_p$.

The imaginary-frequency dipole polarizability $\alpha(i\omega)$ for the He $2\,^3S_1$ atom and the dielectric function of silicon for several conductivities are shown in Fig. 1(a). We calculated the interaction potentials as a function of the distance from the surface by integrating Eq. (1). The result is shown in Fig. 1(b). The potential for a He $2\,^3S_1$ atom and a perfect conductor is shown by the short-dashed line: The curve is calculated with the values for $\alpha(i\omega)$ given in Refs. [31,32] and reproduces the data given by Yan and Babb [26], which are shown as crosses, with a relative error below 1%. The long-dashed line shows the potential between the He atom and a dielectric with $\epsilon(i\omega) = \epsilon(0) = 11.7$, and the solid line the potential cal-
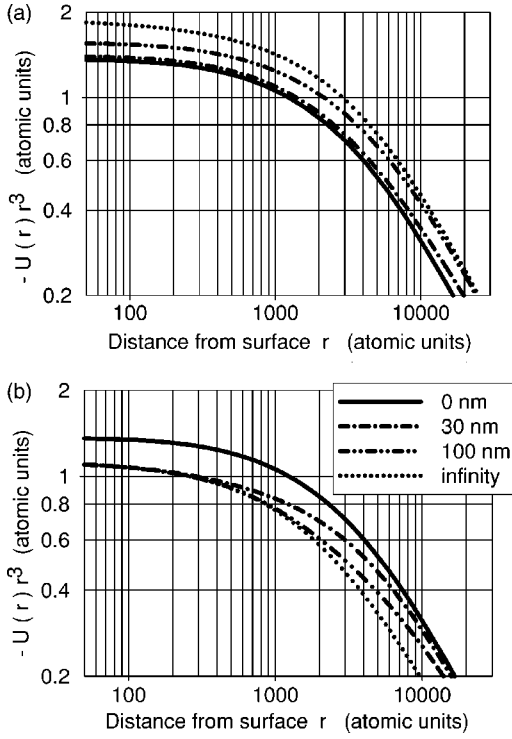
FIG. 2. (a) Demonstration of the effect of the conductivity of a solid on the van der Waals potential in the case of silicon and metastable helium $2\,^3S_1$. The potential for a perfect conductor is shown by the dotted line. The solid line represents the potential for undoped silicon, which behaves like a dielectric. We also show the potential for doped silicon with plasma frequencies $\omega_p=10^{15}$ s^{-1} (dash-dot) and $\omega_p=10^{16}$ s^{-1} (dash-dot-dot). Note that the effect of free charges appears mainly at a larger distance from the surface. (b) The van der Waals potential between a He* atom and a silicon surface covered with an oxide layer. The silicon oxide is assumed to be a dielectric with constant $\epsilon=3.9$. The potentials are shown for undoped silicon (solid line) and layers of thickness of $t=30$ nm (dash-dot), $t=100$ nm (dash-dot-dot), and $t=\infty$ (dotted).

culated with the dielectric function of silicon from Eq. (19). The difference between the two latter curves appears only at short distances from the surface, where the high-frequency behavior of $\alpha(i\omega)$ and $\epsilon(i\omega)$ must be considered.

The dependence of the potential on the conductivity is demonstrated in Fig. 2(a). For illustrative purposes, the potential is shown for the values of the plasma frequency $\omega_p=10^{15}$ and 10^{16}. If we assumed a damping rate of $\gamma_0=10^{13}$ s^{-1} [34] and set the effective mass equal to the electron mass, the corresponding conductivities are about $\sigma_0=10^4$ (Ω cm)$^{-1}$ and $\sigma_0=10^6$ (Ω cm)$^{-1}$, respectively. In practice, such high values are not achievable with doped silicon. At lower conductivities, the potential practically coincides with the pure dielectric case. At higher conductivities and at larger distance, the potential approaches that of a perfect conductor.

VI. THE INFLUENCE OF THE OXIDE LAYER

Silicon samples that have been exposed to air are covered with a thin layer of silicon oxide. The thickness of such naturally grown layers is in the order of a few nanometers, depending on the time of exposure and other conditions. This naturally grown oxide usually consists of some intermediate oxide such as SiO$_x$, rather than SiO$_2$ [35]. In semiconductor device fabrication, silicon wafers are passivated by growing a much thicker layer of several hundred nanometers at higher temperatures [36]. Silicon oxide forms a large variety of structures with different properties, but the naturally grown oxide can generally be considered to be a glass with an index of refraction around 1.5 in the optical region, and a static dielectric constant around 3.9 [34]. Since the dielectric constant of the oxide is much smaller than that of pure silicon, a thin oxide layer is expected to slightly change the shape of the van der Waals potential near the surface. In this section, we discuss the potential generated by a thin layer and quantify the effect of the oxide layer on the van der Waals potential of a silicon surface.

The r^{-3} and r^{-4} dependence of the potential between an atom and a solid surface can be derived via a pairwise summation of the interatomic potential between the atom and all atoms of the solid in the entire half-space. The van der Waals potential between two atoms varies with the interatomic distance as r^{-6}, and as r^{-7} at larger distance due to the retardation of the electromagnetic field. The method of integrating over pairwise interactions reproduces, however, only the correct potential shape; the quantitative agreement is only approximate, because the force between two atoms generally depends on the presence of other atoms. Nevertheless, the method provides useful approximations when the potential for more complicated geometries has to be calculated. Following this idea, we consider the van der Waals potential near a surface to be the result of an integration over the entire volume of the solid, with all interactions included. If the last step of this integration was along the direction perpendicular to the surface, we can write $U(r)=-U(r+s)|_{s=0}^{\infty}$. The potential of a layer of finite thickness is then readily obtained by replacing the integration boundaries.

Assume, for example, that a substrate with van der Waals constant C_3^s is covered with a layer of thickness t of a material with constant C_3^l. Then the potential of the entire surface can be calculated to be $U(r)=-C_3^s(r+t)^{-3}+C_3^l[(r+t)^{-3}-r^{-3}]$. At a distance from the surface $r<t$, the potential shape is determined by the properties of the layer material, whereas at $r>t$ the properties of the substrate material dominate, with a smooth transition between the two regions.

In order to calculate the van der Waals potential of the silicon oxide layer, we assume that the silicon oxide is a dielectric with frequency-independent dielectric constant $\epsilon=3.9$, and we calculate the coefficients as $C_3=C_3^\infty(\epsilon-1)/(\epsilon+1)=7.27\times10^{-49}$ J m^3 and $C_4=C_4^\infty(\epsilon-1)/(\epsilon+1)\phi(\epsilon)=8.04\times10^{-56}$ J m^4 by using Eqs. (6) and (8). The potential of the layer material is then approximated by $U(r)=-C_4/[r^3(r+l)]$ with $l=C_4/C_3$. The calculated potential is shown in Fig. 2(b) for several values of the layer thickness.

It can be seen that even for a thin layer of 30 nm, the potential is reduced by a few percent at a distance of 150 nm (2834 a.u.), where the atoms are reflected in our experiment. Such a thin oxide layer will therefore lead to a small increase of the reflectivity.
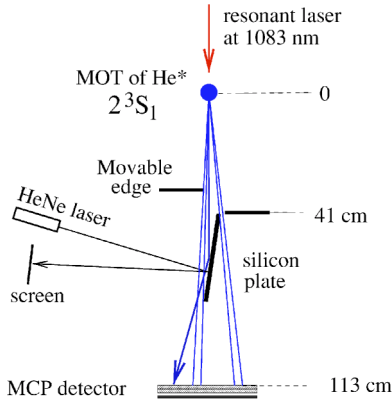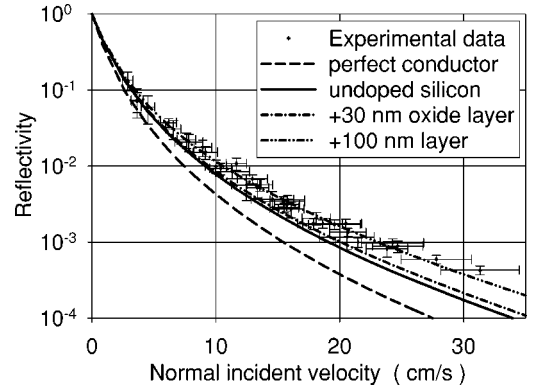
FIG. 3. Cross-sectional view of the experimental setup.

FIG. 4. Measurement of the reflectivity of He* ($2\,^3S_1$) on a polished *p*-doped silicon plate as a function of the normal incident velocity (error bars). We compare the result to the reflectivities calculated for several potentials. The long-dashed line shows the reflectivity expected for He* on a perfect conductor. The solid line shows the case for undoped silicon (i.e., with low conductivity). The reflectivities expected for a Si surface covered with a 30-nm- (dash-dot) and 100-nm-thick (dash-dot-dot) oxide layer are also shown.

Generally, at a layer thickness of several hundred nanometers the reflectivity will be solely determined by the properties of the layer material. Deposition of a low-dielectric constant film will increase the reflectivity, whereas deposition of a metal film will decrease the reflectivity of atoms.

VII. EXPERIMENT

The experimental setup has already been described previously [17]. It is schematically shown in Fig. 3. Metastable helium atoms in the $2\,^3S_1$ state are trapped and cooled in a magneto-optical trap (MOT) using the transition at 1083 nm. The atoms are released from the trap by illuminating the cloud of atoms from the top with short pulses of resonant light. Focusing of the laser beam to a $1/e^2$ waist below 100 μm provides an almost pointlike source of atoms. A silicon plate is placed in the beam line 41 cm below the trap. The plate can be rotated around the upper edge to adjust the incident angle, which was varied between 1.3 and 6.5 mrad. The pattern of scattered atoms is detected with a gated microchannel plate (MCP) detector, placed 113 cm below the MOT. In order to improve the time resolution of the time-of-flight measurement, only atoms that arrive after a chosen delay and within a short interval are detected. We typically reduced the velocity spread to below 10%. The length and intensity of the releasing laser pulses are adjusted to maximize the number of atoms within the chosen interval. The MOT is switched off directly after the releasing pulse as well as during the detection interval.

The pattern on the MCP detector consists of atoms passing behind the silicon plate, atoms passing in front of the silicon plate, and atoms reflected on the plate. A movable edge is placed 4 cm above the silicon plate to block out atoms that would otherwise overlap with the reflected part. The reflected atoms can be clearly distinguished from directly falling atoms down to incident angles of about 1 mrad. The relative angle between the surface and the atomic beam is measured by reflecting a HeNe laser on the silicon plate. The reflectivity is determined as the ratio of the number of atoms in the reflected part and the number of incident atoms, which is determined using the number of atoms passing behind the plate and the projected width of the silicon plate.

We used a $200 \times 20 \times 0.5$ mm silicon plate of B-doped *p*-type, with a conductivity of about 0.02 $(\Omega\,\mathrm{cm})^{-1}$. The (001) surface was covered with a layer of naturally grown silicon oxide. We estimated the thickness of the layer by measuring the reflectivity of a HeNe laser on the sample for various polarizations and incidence angles. The result of this measurement indicates a layer thickness below 10 nm. The surface was polished and is expected to have a roughness in the order of several nm.

We measured the reflectivity on our sample as a function of the normal incident velocity component between 3 and 30 cm/s. Both the parallel incident velocity (23 m/s to 70 m/s) and the incident angle (1.3–6.5 mrad) have been varied to check the consistency of the measurement. An error analysis was done for all data points. The result is shown in Fig. 4.

We compare them to the reflectivity expected for He* atoms reflected on a perfectly conducting surface (dashed) and on a silicon surface with low conductivity that behaves like a dielectric (solid). The curves are obtained by solving the one-dimensional Schrödinger equation with the interaction potentials calculated in Sec. V. As a boundary condition we assume that close to the surface the wave function contains only the wave moving towards the surface. This calculation does not include any short-range interaction, i.e., the potentials considered here are all divergent at $r=0$. Our data are described relatively well by using the potential calculated for the silicon surface that behaves like a dielectric, whereas the curve calculated for a perfect conducting surface clearly deviates from our measurement.

However, the measured reflectivity is slightly larger than expected for undoped silicon. This could in principle be explained by the presence of a thin oxide layer. We show the reflectivities expected for a thickness of 30 and 100 nm in Fig. 4. The deviation of the data would suggest a layer thickness of about 100 nm. However, an independent measurement indicated a thickness of below 10 nm and the effect of such a thin oxide layer on the reflectivity of atoms should be

negligible. The observed deviation might rather indicate that some short-range interaction should be included, in particular at higher incident velocities.

We mentionned above that in our case the de Broglie wavelength ranges from 0.3 to 2 μm, and that the distance of reflection from the surface lies between 150 and 300 nm. This distance is larger than or equal to the distance where retardation is observed, i.e., $r > l = 137$ nm: For low velocities the reflectivity is therefore determined by the retarded potential and for higher velocities by the potential in the transition region. The region of reflection lies near the distance $l = 137$ nm for incident velocities near $v = 38$ cm/s.

We also believe that the reflection is coherent because the de Broglie wavelength and the distance of reflection are large compared to the surface roughness.

VIII. CONFIRMATION OF THE SCALING LAW

The quantum reflection on a silicon surface has been previously studied on the same silicon sample with metastable Ne atoms [8]. This allows us to directly confirm the scaling of the reflectivity with atomic mass. The reflectivities for He and for Ne are shown together in Fig. 5(a).

The ratio of the atomic masses of He and Ne is $M^{Ne}/M^{He} = 5$. Using Eq. (7) and the value for the static dipole polarizability $\alpha^{Ne}(0) = 3.07 \times 10^{-39}$ F m^2 we calculate the constant C_4^∞ for Ne* to be 1.0×10^{-55} J m^4. Similarly, we estimate the constant C_3 for Ne* to be 1.13×10^{-48} J m^3 by using Eq. (16) and the value $\omega_a^{Ne} = 3.1 \times 10^{15}$ s^{-1} [37].

Using Eq. (11), we then obtain the following scaling velocities for He and Ne: $v_s^{He} = 4.89$ cm/s and $v_s^{Ne} = 5.69$ mm/s for the retarded potential, and $v_s^{He} = 2.16$ cm/s and $v_s^{Ne} = 0.94$ mm/s for the unretarded potential. Their ratios are $v_s^{He}/v_s^{He} = 8.6$ for the retarded and $v_s^{He}/v_s^{He} = 23$ for the unretarded potential, respectively.

In Fig. 5(b), we plot the same data as before with the incident velocities scaled by the calculated values for v_s. We use only the values for the retarded potential. After scaling, both sets of data follow nearly the same curve, except at the highest velocities, where the scaling of the unretarded potential (n=3) should be used. The relative increase of the reflectivity due to the smaller mass is even larger for the unretarded potential.

IX. CONCLUSION

In conclusion, we have observed the specular reflection of He* atoms on a flat polished silicon surface and confirm that the reflection is caused by the attractive surface potential tail. This potential, including retardation, has been calculated using the known dipole polarizability of metastable helium and the dielectric function of silicon. For silicon, the van der
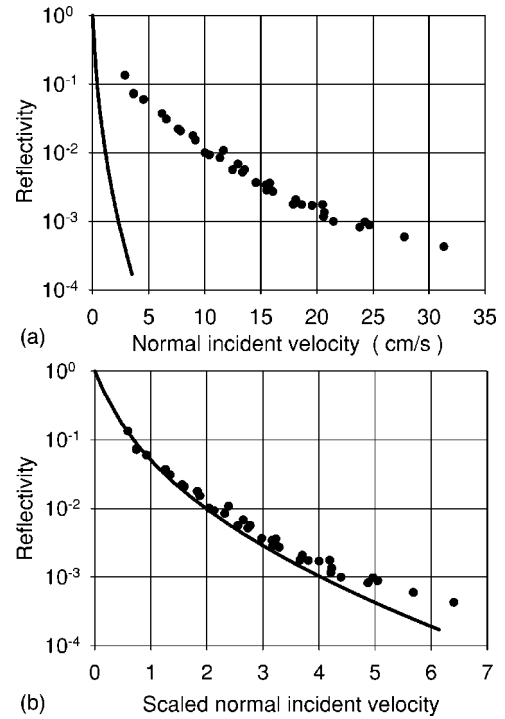

FIG. 5. (a) The reflectivity of He* (points) compared to that of Ne* ($1s_3$) atoms (solid line), both measured on similar silicon samples as a function of the normal incident velocity. The neon data are taken from Ref. [8]. (b) The same data with the normal incident velocities scaled with $v_s^{Ne} = 5.69$ mm/s and $v_s^{He} = 4.89$ cm/s, respectively.

Waals potential is determined by the dielectric properties of the semiconductor, with little influence from the presence of free charges. We also considered the influence of a thin oxide layer on the silicon substrate. For a layer thickness below 20 nm, its effect on the reflectivity of atoms is negligible. Finally, we have compared the reflectivity of He* to that of Ne* measured on the same surface, and confirmed the scaling of the incident velocity with atomic mass and potential parameters.

[1] C. Carraro and M. Cole, Prog. Surf. Sci. **57**, 61 (1998).

[2] R. Doak and A. Chizmeshya, Europhys. Lett. **51**, 381 (2000).

[3] A. Mody, M. Haggerty, J. Doyle, and E. Heller, Phys. Rev. B **64**, 085418 (2001).

[4] V. Nayak, D. Edwards, and N. Masuhara, Phys. Rev. Lett. **50**, 990 (1983).

[5] J. Berkhout *et al.*, Phys. Rev. Lett. **63**, 1689 (1989).

[6] I. Yu *et al.*, Phys. Rev. Lett. **71**, 1589 (1993).

[7] A. Anderson *et al.*, Phys. Rev. A **34**, 3513 (1986).

[8] F. Shimizu, Phys. Rev. Lett. **86**, 987 (2001).

[9] V. Druzhinina and M. DeKieviet, Phys. Rev. Lett. **91**, 193202 (2003).

[10] T. Pasquini *et al.*, Phys. Rev. Lett. **93**, 223201 (2004).

[11] C. Henkel, C. Westbrook, and A. Aspect, J. Opt. Soc. Am. B **13**, 233 (1996).

[12] R. Côté, H. Friedrich, and J. Trost, Phys. Rev. A **56**, 1781 (1997).

[13] H. Friedrich, G. Jacoby, and C. Meister, Phys. Rev. A **65**, 032902 (2002).

[14] X. Halliwell, H. Friedrich, S. Gibson, and K. Baldwin, Opt. Commun. **224**, 89 (2003).

[15] H. Friedrich and A. Jurisch, Phys. Rev. Lett. **92**, 103202 (2004).

[16] F. Shimizu and J. Fujita, J. Phys. Soc. Jpn. **71**, 5 (2002).

[17] H. Oberst, D. Kouznetsov, K. Shimizu, J. Fujita, and F. Shimizu, Phys. Rev. Lett. **94**, 013203 (2005).

[18] R. Eisenschitz and F. London, Z. Phys. **60**, 491 (1930).

[19] J. Lenard-Jones, Trans. Faraday Soc. **28**, 333 (1932).

[20] H. Casimir and D. Polder, Phys. Rev. **73**, 360 (1948).

[21] E. Lifshitz, Sov. Phys. JETP **2**, 73 (1956).

[22] I. Dzyaloshinskii, E. Lifshitz, and L. Pitaevskii, Adv. Phys. **10**, 165 (1961).

[23] V. Parsegian, Mol. Phys. **27**, 1503 (1974).

[24] Y. Tikochinsky and L. Spruch, Phys. Rev. A **48**, 4223 (1993).

[25] Z.-C. Yan, A. Dalgarno, and J. Babb, Phys. Rev. A **55**, 2882 (1997).

[26] Z.-C. Yan and J. Babb, Phys. Rev. A **58**, 1247 (1998).

[27] J. Schwinger, J. L. L. DeRaad, and K. Milton, Ann. Phys. (N.Y.) **115**, 1 (1978).

[28] C. Hargreaves, Proc. K. Ned. Akad. Wet., Ser. B: Phys. Sci. **68**, 231 (1965).

[29] J. Babb, G. Klimchitskaya, and V. Mostepanenko, Phys. Rev. A **70**, 042901 (2004).

[30] J. Jackson, *Classical Electrodynamics*, 3rd ed. (John Wiley & Sons, New York, 1998).

[31] D. Bishop and J. Pipin, Int. J. Quantum Chem. **47**, 129 (1993).

[32] R. Glover and F. Weinhold, J. Chem. Phys. **66**, 191 (1977).

[33] G. Vidali and M. Cole, Surf. Sci. **110**, 10 (1981).

[34] E. D. Palik, *Handbook of Optical Constants of Solids* (Academic Press, Oxford, 1988).

[35] H. Philipp, J. Appl. Phys. **43**, 2835 (1972).

[36] S. Sze, *Semiconductor Devices, Physics and Technology* (John Wiley & Sons, New York, 1985).

[37] R. Brühl *et al.*, Europhys. Lett. **59**, 357 (2002).